Sideslip Estimation of Formula Student Prototype

André Manuel Pinheiro Antunes
andre.antunes@tecnico.ulisboa.pt

Instituto Superior Técnico, Universidade de Lisboa, Lisboa, Portugal

November 2017

Abstract

The objective of this work is the design and tuning of an estimator architecture that can provide the slipangle of a Formula Student prototype, with the requirement of working in real time, to be able to feed a control algorithm. The proposed architecture uses an Inertial Measurement Unit (IMU) composed of an accelerometer a gyroscope and a magnetometer, a Global Positioning System (GPS), a steering encoder, the torque of the electrical motors and the underlying dynamic model of the vehicle. An exhaustive car model is presented, as well as, sensor models, used to test and tune the estimators. Two kinematic complementary filters are presented for attitude and velocity estimation that feed a third estimator using the vehicle dynamics. For this last one, a linear and a non-linear filter are compared and their pros and cons discussed. All the used estimators are based in Kalman Filter (KF) theory for the linear ones and the Extended Kalman Filter (EKF) for the non-linear. The estimator architecture is then tested with offline data from a real Formula Student prototype. The test is cross-validated with a secondary and more accurate system.
Keywords: Sideslip, Navigation, Estimation, Sensors, Kalman Filter

Introduction

Formula Student is an university competition that challenge students from around the world to build a single-seat racing car. Along the years the competition has been evolving with the implementation of new materials and technologies, always looking to follow the world evolution of automotive technology. Recently it has approach the driverless cars starting a new parallel competition for these vehicles, which associated with electric independent all-wheel drive already used by the teams, opens a door for countless control approaches. Control strategies like vehicle stability control and torque-vectoring [1] depend widely on a sideslip observer to assure that the vehicle stays in a stable route. This observer is especially needed when there are significant differences between the model and the true vehicle, something that usually happens when working with road vehicles and tyres.

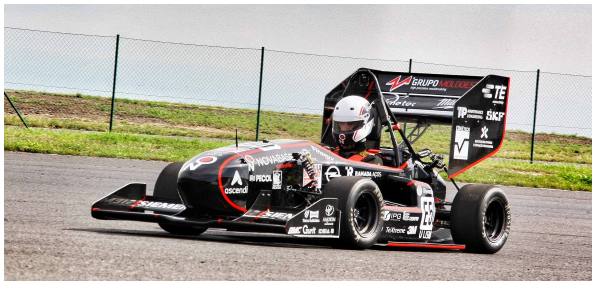

Figure 1: IST - FST06e

This paper undertakes the implementation of an architecture proposed in [2] for a Formula Student prototype to estimate the sideslip of the vehicle. During a test day, data was acquired from an inertial measurement unit (IMU) consisting of an accelerometer a magnetometer and a gyroscope, all of them with 3 axis, a global positioning system (GPS) and a steering encoder. These sensors were already part of the vehicle. In order to verify the results obtained from the estimators, a secondary system using a differential global positioning system (DGPS) was attached to the car. This one gives the heading and the velocity components, values required to calculate the sideslip angle of the car. Both systems, the DGPS and the car sensors are completely independent. The acquired values are then processed in offline to skip implementation issues.

In this document, the models and estimators are briefly explained in sections 2 and 3 respectively, with only the more important equations presented, their deduction can be found in [2] and [3]; followed by a closer look to the test platform (Fig.1), its technical characteristics, and the sensors are explored in section 4; Section 5 illustrates the results obtained in each estimator and a comparison is performed with the values from the DGPS; Finally, Section 6

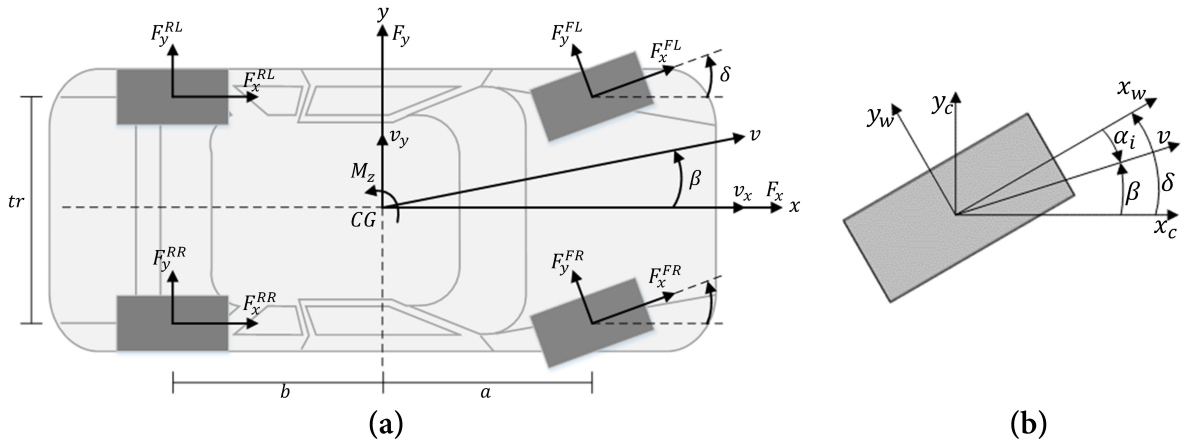

Figure 2: (a)Forces applied on the Car; (b)Tyre angles and frames. Images from [2]

outlines some remarks and future work.

Car Model

This section presents the general non-linear equations for the vehicle model from where the linear car model is obtained. These equations and their deduction are explored in detail by [2], and as such, in this work only the resulting equations are exposed.

The following model is named a planar model since it considers that no pith (θ) or roll (ϕ) rotations exist, being these the major assumptions, which also implies that no load transfer occurs. Besides this limitation, aerodynamics forces acting on the car are neglected. This restricts all the forces to the tyres, as can be seen in Fig.2(a), where each one produces a longitudinal and a lateral force respectively F_x and F_y, with the indexation Front Left (FL), Front Right (FR), Rear Left (RL) and Rear Right (RR). And where δ defines the wheel steer angle, v is the velocity vector, β is the car sideslip angle, a is the distance between the centre of gravity (CG) and the front axle, b the distance between the CG and the rear axle, and tr is the length of the axle, where both are considered equal.

The resulting equations of this model are described by (1), where r is the angular velocity around the z-axis, m is the mass of the car plus the driver and I_z is the moment of inertia around the z-axis.

$$\dot{v}_x = v_y r - \frac{1}{m}[F_y^F \sin\delta - F_x^R] \tag{1a}$$

$$\dot{v}_y = -v_x r + \frac{1}{m}[F_y^F \cos\delta + F_y^R] \tag{1b}$$

$$\dot{r}_z = \frac{1}{I_z} a F_y^F \cos\delta - \frac{1}{I_z} b F_y^R \tag{1c}$$

The longitudinal force F_x on the car is assumed to be a direct input, without considering the tyres limitations. The lateral forces F_y on the tyres are given by a cornering stiffness approximation expressed by (2), where C_α is the cornering stiffness constant, and α_i is the slip angle of the tyre i, defined as $\alpha_i = \beta_i - \delta_i$, as seen in Fig.2(b).

$$F_y = -C_\alpha \alpha_i \tag{2}$$

The sideslip angle of the wheel (β_i) is the projection of the sideslip angle β of the car in the wheel by $v_i = {}^B v + {}^B r \times {}^B \boldsymbol{r}_i$, where ${}^B \boldsymbol{r}_i$ is the vector of distance between the CG and the wheel i. This cornering stiffness approximation contains several assumptions that are explained in detail in [2].

Linear Car Model

The car model used in the estimator is an approximation of the equations (1) and (2) for small angles and the assumption of a constant longitudinal velocity ($v_x = const$), which has been widely used in the literature [4][5][6]. With the small angle approximation is possible to define the wheel slip angle as:

$$\alpha_i = \text{tg}^{-1}\left(\frac{v_y + x_i r}{v_x - y_i r}\right) - \delta_i \approx \frac{v_y + x_i r}{v_x} - \delta_i \tag{3}$$

Using a different cornering stiffness for front and rear wheels, respectively $C_{\alpha f}$ and $C_{\alpha r}$, is then possible to rewrite (1)-(3) in a state space form:

$$\begin{bmatrix}\dot{v}_y \\ \dot{r}\end{bmatrix} = \begin{bmatrix} -\frac{C_{\alpha f}+C_{\alpha r}}{v_x m} & \frac{-aC_{\alpha f}+bC_{\alpha r}}{v_x m} - v_x \\ \frac{-aC_{\alpha f}+bC_{\alpha r}}{I_z v_x} & -\frac{a^2 C_{\alpha f}-b^2 C_{\alpha r}}{I_z v_x}\end{bmatrix}\begin{bmatrix} v_y \\ r\end{bmatrix} + \begin{bmatrix}\frac{C_{\alpha f}}{m} \\ \frac{aC_{\alpha f}}{I_z}\end{bmatrix}\delta \tag{4}$$

Estimator Architecture

In this section, the proposed architecture for the estimation of the sideslip is exposed. As depicted in Fig.3, the estimation process is composed of three

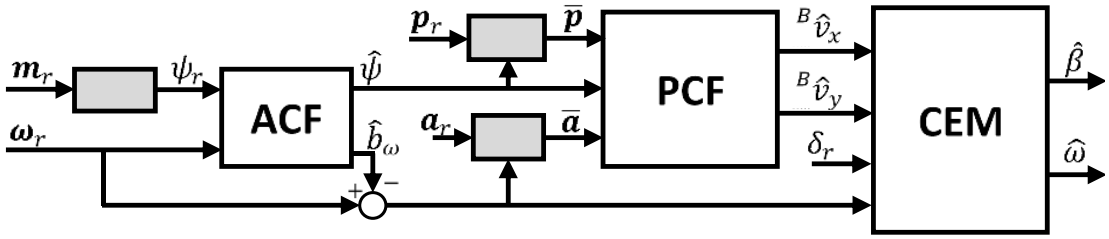

Figure 3: Flowchart of Filter Scheme where $\mathbf{m}_r$, ω_r, $\mathbf{a}_r$, $\mathbf{p}_r$ and δ_r are respectively the reading from the magnetometer, gyroscope, accelerometer, GPS and steering encoder. Grey boxes represent required data processing before use in filters.

sequential filters. An Attitude Complementary Filter (ACF), a Position Complementary Filter (PCF), and a Car Estimation Model (CEM).

The ACF is used to correct the yaw reading from the magnetometer and to estimate the bias of the gyroscope. The yaw is then used in the rotation matrices inside the PCF, which uses the accelerometer and the GPS to estimate both velocity components in the body reference frame. The CEM is used to include the car dynamics in the sideslip estimation using the velocity components, the corrected yaw rate and the steering angle. The three filters are implemented using discrete Kalman Filter [7][8], where the CEM is discretized from a continuous state space model. Both complementary filters are explained in more detail in [2] and [3].

Attitude Complementary Filter

The ACF combines the yaw readings with the angular velocity around the z-axis to give a more accurate yaw value and a bias estimation for the angular velocity to correct the gyroscope signal. This assumes that the yaw rate $\dot{\psi} = \omega_{r,k}$ reading is affected by random white noise ($w_{\omega_r,k}$) as well as a constant bias ($b_{\omega k}$):

$$\omega_{rk} = \omega_k + b_{\omega k} + w_{\omega_r,k}$$

With this, is then possible to write the discrete Kalman Filter in a state space form as:

$$\begin{bmatrix}\psi_{k+1}\\ b_{\omega k+1}\end{bmatrix} = \begin{bmatrix}1 & -T\\ 0 & 1\end{bmatrix}\begin{bmatrix}\psi_k\\ b_{\omega k}\end{bmatrix} + \begin{bmatrix}T\\ 0\end{bmatrix}\omega_{r,k} + \begin{bmatrix}K_1\\ K_2\end{bmatrix}(y_k - \hat{y}_k)$$

$$\hat{y}_k = \hat{\psi}_k\ , \qquad y_k = \psi_{r,k} + v_k$$

where the index k defines the instant in time $t = kT$ being T the sampling time interval. The gyroscope reading is $\omega_{r,k}$, and the yaw reading from the magnetometer is $\psi_{r,k}$ which is corrupted with random white noise v_k. The values K_1 and K_2 are the Kalman gains associated to each state.

Position Complementary Filter

The PCF combines the readings of the accelerometer with the ones from the GPS to give an estimate of the velocity components in the vehicle body frame which in this case are unobservable states. Since the GPS uses a global reference frame as the opposite of the accelerometer and the needed velocity components, the yaw estimation from the ACF is used to convert between reference frames using a rotation matrix defined as R_k. The equations that rule the PCF are the motion equations:

$$\bar{\mathbf{p}}_{k+1} = \bar{\mathbf{p}}_k + T\bar{\mathbf{v}}_k + \frac{T^2}{2}\mathcal{R}_k\bar{\mathbf{a}}_k$$

$$\bar{\mathbf{v}}_{k+1} = \bar{\mathbf{v}}_k + T\mathcal{R}_k\bar{\mathbf{a}}_k$$

where $\bar{\mathbf{p}}$, $\bar{\mathbf{v}}$, $\bar{\mathbf{a}}$ are respectively the vectors of position, velocity and acceleration. Is then possible to write the PCF system as:

$$\begin{bmatrix}\hat{\mathbf{p}}_{k+1}\\ {}^B\hat{\mathbf{v}}_{k+1}\end{bmatrix} = \begin{bmatrix}I & T\bar{\mathcal{R}}_k\\ 0 & I\end{bmatrix}\begin{bmatrix}\hat{\mathbf{p}}_k\\ {}^B\hat{\mathbf{v}}_k\end{bmatrix} + \begin{bmatrix}\frac{T^2}{2}\bar{\mathcal{R}}_k\\ TI\end{bmatrix}\bar{\mathbf{a}}_k + \begin{bmatrix}K_{1p}\\ \bar{\mathcal{R}}_k' K_{2p}\end{bmatrix}(\mathbf{y}_{pk} - \hat{\mathbf{y}}_{pk})$$

$$\hat{\mathbf{y}}_{pk} = \hat{\mathbf{p}}_k\ , \quad \mathbf{y}_{pk} = \bar{\mathbf{p}}_k + \mathbf{v}_{pk}$$

where $I \in \mathbb{R}^2$ is the identity matrix, $\bar{\mathbf{a}}_k$ is the readings from the accelerometer, $\bar{\mathbf{p}}_k$ is the GPS readings of position that are corrupted with random white noise $\mathbf{v}_{pk}$. The values K_1 and K_2 are 2×2 diagonal matrices with the Kalman gains identified with a linear time-invariant system based on the above, explored in [2] and [3]. The subscript B indicates the components in the vehicle body frame.

Car Estimator Model

The Car Estimator Model is based on system (4), which depends on two state variables $[v_y\ r]$. This system is time variant due to v_x, which can generate complications if the longitudinal velocity is zero, or close to zero due to numeric problems. The CEM uses the velocity components estimations of

Table 1: FST06e Parameters

Description	Var	Variable	Units
Front and rear track	–	1.24	m
Mass of the Car + Driver	m	356	kg
Yaw Inertia	I_z	120	$kg.m^2$
Weight distribution	–	$45.1 - 54.9$	$\% - \%$
Static load at front wheels	${}^F F_z$	787.5	N
Static load at rear wheels	${}^R F_z$	958.7	N
Cornering Stiffness front	$C_{\alpha f}$	1.527×10^4	N/rad
Cornering Stiffness rear	$C_{\alpha r}$	1.995×10^4	N/rad

the PCF, the gyroscope reading corrected with the bias from the ACF, and the steering angle of the wheel. The system for the filter is given by:

$$\begin{bmatrix}\dot{\hat{v}}_y \\ \dot{\hat{r}}\end{bmatrix} = \begin{bmatrix} -\frac{C_{\alpha f}+C_{\alpha r}}{v_x m} & \frac{-aC_{\alpha f}+bC_{\alpha r}}{v_x m} - v_x \\ \frac{-aC_{\alpha f}+bC_{\alpha r}}{I_z v_x} & -\frac{a^2 C_{\alpha f}-b^2 C_{\alpha r}}{I_z v_x}\end{bmatrix}\begin{bmatrix}\hat{v_y} \\ \hat{r}\end{bmatrix} + \begin{bmatrix}\frac{C_{\alpha f}}{m} \\ \frac{aC_{\alpha f}}{I_z}\end{bmatrix}\delta + \begin{bmatrix}K_{1v_y} & K_{1r} \\ K_{2v_y} & K_{2r}\end{bmatrix}(y_l - \hat{y}_l)$$

$$\hat{y}_l = \begin{bmatrix}\hat{v_y} \\ \hat{r}\end{bmatrix}, \quad y_l = \begin{bmatrix}v_y \\ r\end{bmatrix} + \begin{bmatrix}\mathbf{v}_{v_y} \\ \mathbf{v}_r\end{bmatrix}$$

where $\mathbf{v}_{v_y}$ and $\mathbf{v}_r$ are the noises associated to each measurement and the K_i gains are the Kalman gains that relate the error of measured and estimated data to each state variable.

Test Platform

In order to test the proposed estimation architecture, a real test was conducted. At the time, these algorithms weren't already implemented in a hardware capable of real-time processing, so all the data was logged, and processed offline after the test. The test platform was FST06e (Fig.1), an electric Formula Student Prototype. This vehicle is propelled by two independent 50kW motors at the rear, one motor per wheel, with a single fixed gear with no clutch. With a weight of 280Kg and a distance between axis of 1.59m, is capable of achieve 0-100Km/h in 2.9s, and a top speed of 150km/h. The remaining parameters of the car needed for the models and estimators are presented in Tab.1.

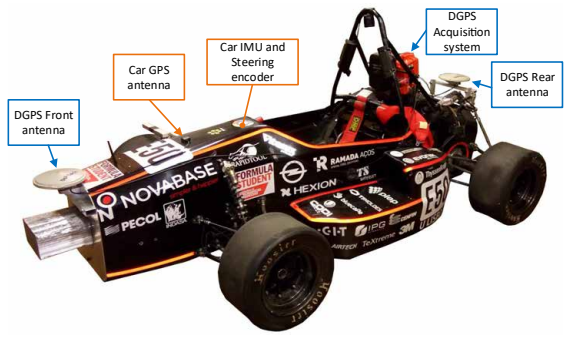

Figure 4: FST06e Acquisition system with DGPS. In orange are the sensors belonging to the car, and in blue the elements of the DGPS.

The car relies on a distributed electronic circuit for all the monitoring, controls and acquisition. This circuit spreads all along the car, and consists in several modules interconnected by a CAN-BUS line working at $1Mbit/s$. For this test 3 modules were essential, the GPS, the Steering and IMU, and the log unit. Each of these modules has one dedicated micro-controller, a dsPIC30f4013 from Texas Instruments, working at $30MHz$ in a self-developed board. The GPS module incorporates a SkyTraq S1216F8 chip configured to an update rate of $25Hz$. The Steering and IMU module consists of a GY-80 IMU that includes a 3-axis accelerometer (ADXL345), a 3-axis gyroscope (L3G4200D) and a 3-axis magnetometer (HMC5883L). The steering encoder is a 3-turn rotational potentiometer used as a voltage divider with a 12bit ADC, that is attached to the steering column. The log unit simply reads one message at the time in the CAN-BUS line and writes it to a file in an SD card.

In order verify the estimated data, a second independent system was used. This one, wasn't connected to the car's previous system, and had a separated log system. This system consisted of two GPS antennas placed on the front and rear of the car separated by 2.5m as seen in Fig.4. The antennas were connected to an Ashtech MB100 board that can deliver the heading angle and velocity components needed to calculate the sideslip angle of the car. This data was logged at $10Hz$.
The acquisition was made during a track day at the university campus using a parking lot limited to an asphalt area of approximated $60m \times 25m$. The trajectory of the car consisted in several circles in both ways, and turns after a long straight.

Results

This section presents the results from the different filters and estimators during the test run using the FST06e with the DGPS (Fig.4). Is also ex-

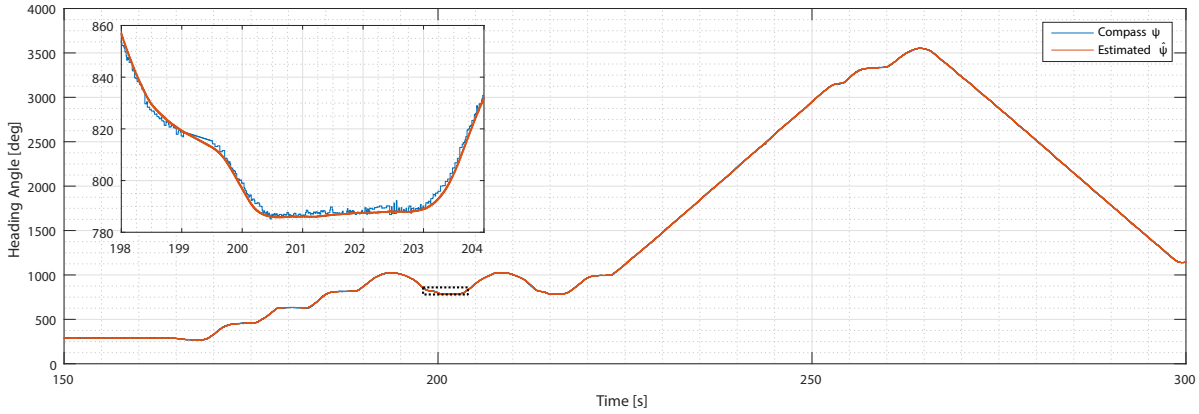

Figure 5: ACF heading angle result and raw heading measurement from the magnetometer.

plained the processing done to each signal before the filters.

For this test, the car was stripped of all aerodynamic elements, to better correspond to the models, and for the antennas to have a clean view of the sky.

Attitude Complementary Filter

To feed the Attitude complementary filter, the data from gyroscope and the magnetometer are required. Before the use of this data, a calibration to align the axis of the IMU with the vehicle axis is done using the accelerometer with data from a static acquisition. This calibration is used in the three sensor units (accelerometer, gyroscope and magnetometer), and kept for all the filters. The yaw angle is computed from the magnetometer after a 3-dimensional calibration is done to correct hard and soft non-linearities [9]. The yaw angle is also corrected from the magnetic declination, to match the position referential.

The ACF is fed with this data resulting in a corrected yaw angle of the vehicle as can be seen in Fig.5. The angle must be in a continuous or cumulative form, since discontinuities in the transition from $0° \leftrightarrow 360°$ or $-180° \leftrightarrow 180°$ generate problems in the ACF. In Fig.5, is possible to see the estimated heading angle of the car, side by side with the raw value from the magnetometer. Besides the yaw angle, also the bias of the gyroscope's z-axis is estimated. In Fig.6, an overlapping of several responses to different initial conditions are presented, showing a convergence after some seconds. From the analysis of the raw data of the sensor, an offset of $-0.62°/s$ was expected for a stationary measurement, something that is verified in the graph.

Analysing Fig.6, is possible to see that around the $160s$, the bias starts to oscillate. This is when the vehicle started to move. One of the assumptions made at the start is that no roll or pitch happens, but in the real vehicle this isn't true. Although

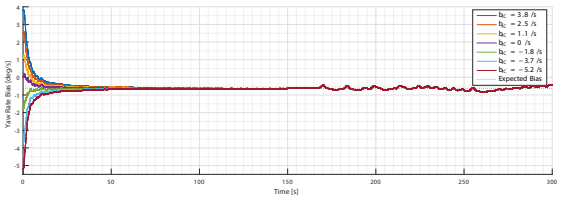

Figure 6: Bias result from the ACF, and a overlapping of several responses for different initial conditions

small, these rotations exist and influence the IMU that is attached to the car. Besides that, the track isn't perfectly flat containing a slight tilt in one side. These unpredicted rotations can justify the oscillations when the car is moving.

Position Complementary Filter

The position complementary filter relies on three major sources, the GPS, the accelerometer and the corrected yaw angle or heading of the car from the ACF. A GPS receiver doesn't give the required X and Y position coordinates, so a transformation is done from ECEF (Earth-Centred, Earth-Fixed) coordinates to ENU (East North Up) coordinates, using as origin a point along the track. The East is defined as the X coordinate, and North the Y coordinate, the Up or Z is not used. Also, a correction is performed to the location of the GPS antenna, this was considered necessary since the distance between the antenna and the centre of gravity was substantial ($\approx 1m$). The correction was performed using (5) where $\bar{\mathbf{d}}_{gps}$ is the vector with the distance from the GPS antenna to the centre of gravity, and ψ is the yaw angle from the ACF.

$$\begin{bmatrix} x_{cg} \\ y_{cg} \end{bmatrix} = \begin{bmatrix} x_{gps} \\ y_{gps} \end{bmatrix} + \begin{bmatrix} \cos\psi & -\sin\psi \\ \sin\psi & \cos\psi \end{bmatrix} \bar{\mathbf{d}}_{gps} \quad (5)$$

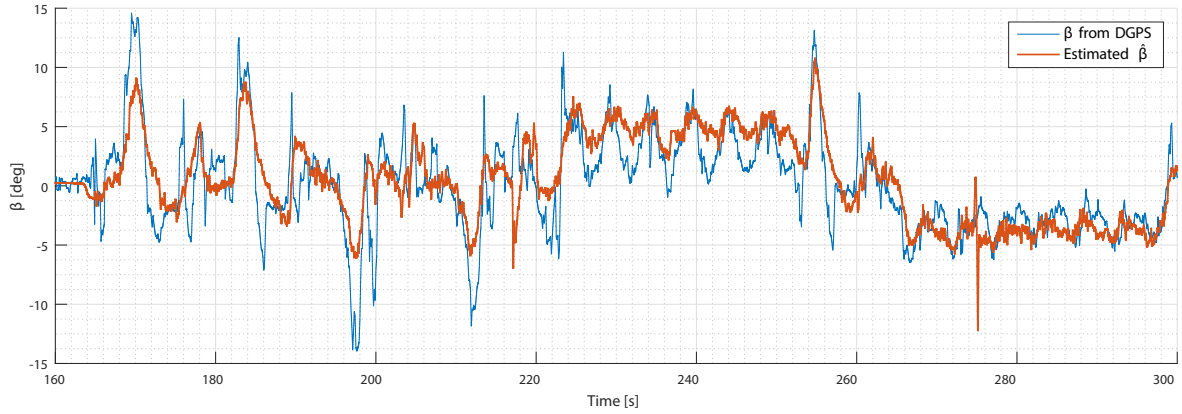

Figure 7: Sideslip angle (β) estimation from the CEM compared with the one given by the DGPS

The GPS only has a $25Hz$ acquisition frequency compared with the $100Hz$ of the remaining sensors, this was overcome by using an interpolation for the missing points to match the general frequency, and was only possible because processing was done offline. For an online application, a multi-rate solution must be implemented, or the global frequency reduced to match the smallest frequency available.

The accelerometer kept the axis calibration explained in the ACF section, and was corrected from offsets in the readings. It was also implemented a correction from the influences of angular velocities due to the distance between the IMU and the centre of gravity using equation (6) where $\bar{\mathbf{A}}_{imu}$ is the vector of accelerations of the reading, $\bar{\mathbf{A}}_{cg}$ is the vector of accelerations in the centre of gravity, $\bar{\omega}$ is the vector of angular velocities, and $\bar{\mathbf{d}}_{imu}$ the distance vector from the IMU to the centre of gravity.

$$\bar{\mathbf{A}}_{imu} = \bar{\mathbf{A}}_{cg} + \bar{\omega} \times (\bar{\omega} \times \bar{\mathbf{d}}_{imu}) \tag{6}$$

The results of the PCF using the values of position acceleration and yaw angle can be seen in Fig.8. This graph presents an overlapping of the velocity components acquired from the DGPS, and

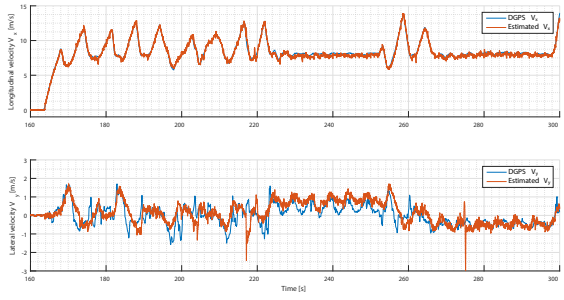

Figure 8: Velocity components estimations resulting from the PCF compared with the ones from the DGPS.

the estimates from the PCF. It must be noticed that the PCF doesn't use in anyway the data from the DGPS, being the two signals completely independent one from the other. The noise is clearly higher in the estimation, this is due to the sensor signals, specially the accelerometer. Since the accelerometer is corrected with the gyroscope unfiltered data using (6), the combination of both signals results in a very noisy signal. An example is the time window between $[225s; 250s]$, where the vehicle was performing several turns at constant radius and speed, and the resulting lateral acceleration from (6) has a mean value of $10.2m/s^2$ and a standard deviation $\sigma = 1.8m/s^2$. In the overall, even with the noise, the estimation of both velocity components is considerably close to the results from the DGPS with small errors.

Car Estimation Model

For this estimator, is necessary the velocity components from the PCF, the steering angle of the front wheels, and the corrected gyroscope reading. The steering encoder mentioned before doesn't read the δ value of the wheel, but the steering wheel angle, besides that, the encoder to achieve a greater resolution relies on a gear ratio to convert the steering wheel range to make a better use of the 3-turn encoder. Due to Ackerman geometry [10] both wheels rarely have the same angle, and the ratio between the steering wheel angle and the wheel angle isn't linear, but for the sake of simplicity this angle is assumed linear and equal. The linear car estimator, uses equation (4) where the transition matrix relies on the longitudinal velocity v_x. For values equal or close to 0, some problems arise since some of the elements are dividing by zero. To overcome this situation, is assumed that the longitudinal velocity used in the transition matrix of (4), has a lower saturation of $v_x = 3m/s$.

A similar problem arises computing

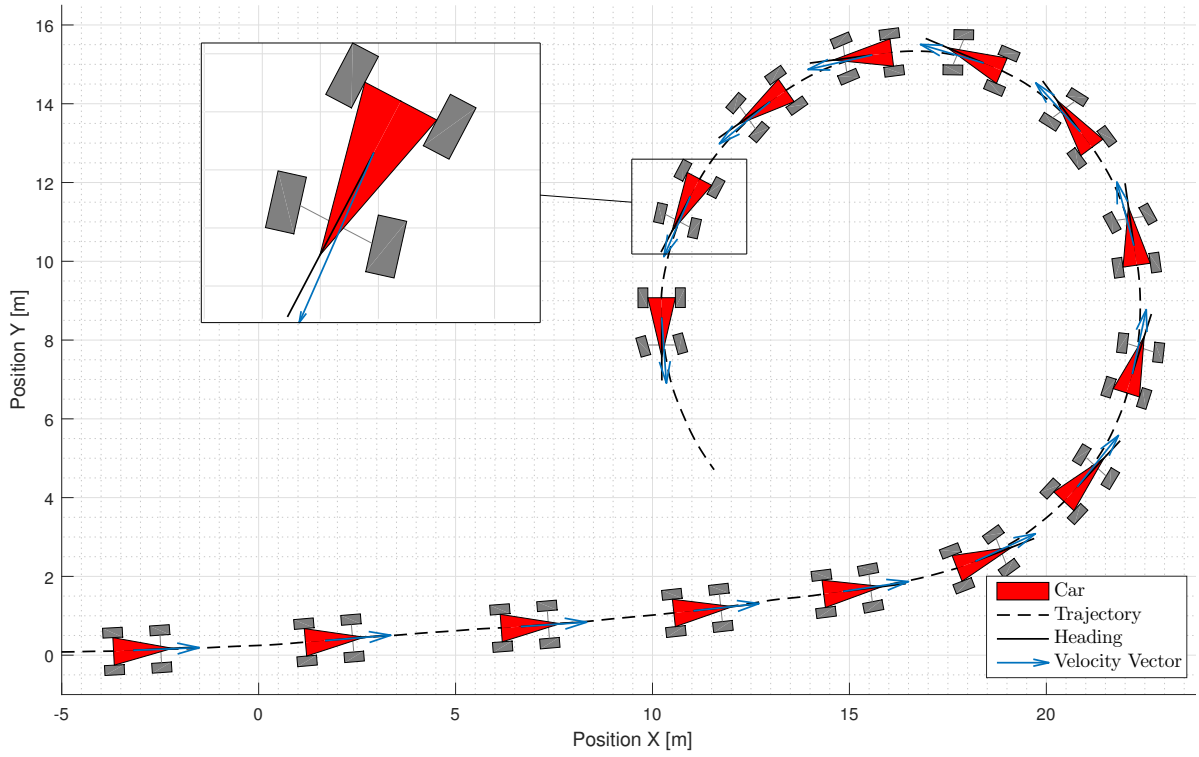

Figure 9: Graphic representation of the results obtained from the estimators with the car represented by a triangle with the heading orientation, and a blue vector representing the velocity vector.

$\beta = \text{tg}^{-1}(v_y/v_x)$ when the velocities are very close to zero, any small noise can generate huge angles. To get around this situation a rule was implemented that when $v_x < 3m/s$ then $v_y = 0m/s$, which means that for small velocities (under $3m/s$) no sideslip occurs. Note that $3m/s$ was just a value that seems small enough to not induce a great error, and worked well during the tests.

The results obtained using the car model estimator for the sideslip angle are presented in Fig.7, as well as the sideslip angle measured by the DGPS. This last one didn't use any signal treatment, and is acquired at only $10Hz$. The resulting signal is a bit noisy due to the input signals, in this case the velocity components from the PCF, as seen previously. Once again, the estimator doesn't use any value from the DGPS. Analysing both signals is possible that the estimative is a little more conservative in terms of amplitude of the angle. With some simple changes in the gains is possible to increase this amplitude, but with the consequence of an increase in the noise. The presented result is a compromise between accuracy and noise. It's also important to remember that one of the assumptions in this filter is the small angle approximation, which from the DGPS values, was clearly exceeded. Even with some differences the estimator keeps up with all the variations registered by the DGPS.

In Fig.9 is possible to see a graphical representation of the car during a part of the track ($[221s; 227s]$), where the car is simplified by a red triangle allign with the heading angle. A blue arrow represents the velocity vector of the car at the centre of gravity. The β, is the angle between the heading and the velocity vector. It's a well-known fact, among all the drivers of this car, that it suffers a lot from understeer, something visible in Fig.9, where is possible to see that the velocity vector always points to the inside of the curve in relation to the heading, showing that behaviour. This situation was also clearly visible during the data acquisition.

Conclusion

The estimation architecture explored was validated on a Formula Student prototype. The Attitude Complementary Filter was implemented with interesting results of heading and an estimate that corresponds to the expected bias. The results of the Position Complementary Filter were close to the ground truth given the low-cost sensors used. The Car Estimation Model was able to produce a sideslip estimation close to the values acquired from the DGPS, and the observed during the field tests. The final results were similar to the values from the DGPS. Thus, the estimation architecture pro-

posed is capable to produce the intended results. This architecture paves the way for the next stages of the projects, namely control system design and driverless competition prototype development, by providing an observer for the sideslip.

References

[1] Leonardo De Novellis, Aldo Sorniotti, Patrick Gruber, and Andrew Pennycott. Comparison of feedback control techniques for torque-vectoring control of fully electric vehicles. *IEEE Transactions on Vehicular Technology*, 63(8):3612–3623, 2014.

[2] André Antunes, Carlos Cardeira, and Paulo Oliveira. Sideslip estimation of formula student prototype through GPS/INS fusion. In *IEEE International Conference on Autonomous Robot Systems and Competitions (ICARSC)*, pages 184–191. IEEE, 2017.

[3] Jos F. Vasconcelos, Bruno Cardeira, Paulo Oliveira, and Pedro Batista. Discrete-time complementary filters for attitude and position estimation: Design, analysis and experimental validation. *IEEE Transactions on Control Systems Technology*, 19(1):181–198, January 2011.

[4] Reza N. Jazar. *Vehicle Dynamics: Theory and Applications*. Springer, 1^{st} edition, 2008. ISBN:978-0387742434.

[5] David Bevly, Jihan Ryu, and J. Gerdes. Integrating ins sensors with gps measurements for continuous estimation of vehicle sideslip, roll, and tire cornering stiffness. *IEEE Transactions on Intelligent Transportation Systems*, 7(4):483–493, December 2006.

[6] Kanghyun Nam, Sehoon Oh, Hiroshi Fujimoto, and Yoichi Hori. Estimation of sideslip and roll angles of electric vehicles using lateral tire force sensors through rls and kalman filter approaches. *IEEE Transactions on Industrial Electronics*, 60(3):988–1000, March 2013.

[7] Gene F Franklin, J David Powell, and Michael L Workman. *Digital control of dynamic systems*, pages 389–391. Addison-wesley Menlo Park, CA, 3^{rd} edition, 1998.

[8] Robert Grover Brown and Patrick Hwang. *Introduction to random signals and applied Kalman filtering: with MATLAB exercises*. Wiley, 4^{th} edition, 2012. ISBN:978-0470609699.

[9] J. Vasconcelos, G. Elkaim, C. Silvestre, P. Oliveira, and B. Cardeira. Geometric approach to strapdown magnetometer calibration in sensor frame. *IEEE Transactions on Aerospace and Electronic Systems*, 47(2):1293–1306, April 2011.

[10] Masato Abe. *Vehicle handling dynamics: theory and application*, pages 5–117. Butterworth-Heinemann, 1^{st} edition, 2009.